Inorganic Chemistry
Article

Inorg. Chem. **2010**, *49*, 2639–2648 **2639**
DOI: 10.1021/ic9014064

Evaluating Binuclear Copper(II) Complexes for Glycoside Hydrolysis

Susanne Striegler,* Natasha A. Dunaway, Moses G. Gichinga, James D. Barnett, and Anna-Gay D. Nelson

Department of Chemistry and Biochemistry, 179 Chemistry Building, Auburn University, Auburn, Alabama 36849

Received July 17, 2009

Three binuclear copper(II) complexes were characterized as solids by X-ray diffraction and in solution by UV/vis spectrophotometric titration, and subsequently evaluated for their glycosidase-like activity. The structure analysis revealed comparable intermetallic Cu···Cu distances (~3.5 Å) for the complexes **2** and **3**. Despite this similarity, the composition of the complexes differs significantly in aqueous solution as revealed by spectrophotometric titrations. The hydrolysis of selected nitrophenylglycopyranosides is up to 11,000-fold accelerated over background in the presence of the copper(II) complexes in 3-(cyclohexylamino)-1-propanesulfonic acid (CAPS) buffer at pH 10.5 and 30 °C.

Introduction

In recent years, several artificial enzyme mimics for glycoside hydrolysis have been studied to model the glycosyl transfer reaction observed in Nature.[1−6] The importance of this reaction is evidenced by the fact that around two-thirds of the carbon in the biosphere exists in the form of carbohydrates. Application of glycosyl transfer reactions is particularly interesting for the synthesis of non-natural carbohydrate entities which are sorely needed as antiviral agents, food fillers, or new antibiotics circumventing the observed increased bacterial resistance to currently available drugs. Although a glycosyl transfer is conveniently achieved with glycosyl transferases, the use of these enzymes is mostly restricted by their limited availability.[7] Glycosidases used as substitutes often lack selectivity and/or provide low reaction yields.

Extensive studies aimed at overcoming these shortcomings with artificial enzyme mimics have employed cyclodextrins derivatized with dicyanohydrins,[2,5] diacids,[6] or trifluoromethyl groups.[1] Although these catalysts show many desirable properties as functional enzyme mimics, they also require elevated temperatures for catalysis,[4] tend to decompose during the reaction, and/or lack catalytic activity when altering the model substrate from a 4-nitrophenyl-glycoside to a 2-nitrophenyl analogue.[3,6] Thus, other catalytic systems with broader applicability are still needed.

Metal ions including Cu(II), Ni(II), Co(II), Al(III), and La(III) have been shown to accelerate the cleavage of disaccharides and other glycosides efficiently.[8,9] So far, studies on the hydrolysis of glycosides using metal ions have largely focused on substrates that provide a binding site for the metal ion close to the glycosidic bond to allow a nucleophilic attack of water on the anomeric carbon. This strategy, however, narrows the pool of substrates to glycosides with strong metal ligating properties and excludes many naturally occurring glycosides, such as disaccharides and oligosaccharides. As a result, a *selective* cleavage of a specific glycosidic bond in substrates that do not possess such strong metal ion ligating properties is out of reach with the currently available methods.

We therefore investigated the use of binuclear transition metal complexes with defined geometry as new tools for the cleavage of glycosidic bonds to open a new direction toward the development of selective artificial glycosidase mimics. For the initial catalyst design, we focused on the evaluation of the structure−activity relationship for binuclear copper(II) complexes with similar pentadentate backbone ligands. The study summarized herein discloses preliminary results on their structures in the solid state, their composition in aqueous solution, and the evaluation of the catalytic hydrolysis of model aryl glycosides in water. A water-soluble pyridine carboxaldehyde-based complex *N*,*N*′-{1,3-bis[(pyridin-2-ylmethyl)amino]propan-2-ol}ato dicopper(II) (μ-acetato)

*To whom correspondence should be addressed. E-mail: susanne.striegler@auburn.edu.

(1) Bjerre, J.; Fenger, T. H.; Marinescu, L. G.; Bols, M. *Eur. J. Org. Chem.* **2007**, No. 4, 704–710.
(2) Bjerre, J.; Nielsen, E. H.; Bols, M. *Eur. J. Org. Chem.* **2008**, No. 4, 745–752.
(3) Ortega-Caballero, F.; Bols, M. *Can. J. Chem.* **2006**, *84*(4), 650–658.
(4) Ortega-Caballero, F.; Bjerre, J.; Laustsen, L. S.; Bols, M. *J. Org. Chem.* **2005**, *70*(18), 7217–7226.
(5) Ortega-Caballero, F.; Rousseau, C.; Christensen, B.; Petersen, T. E.; Bols, M. *J. Am. Chem. Soc.* **2005**, *127*(10), 3238–3239.
(6) Rousseau, C.; Nielsen, N.; Bols, M. *Tetrahedron Lett.* **2004**, *45*(47), 8709–8711.
(7) Khan, S. H.; O'Neill, R. A. *Modern methods in carbohydrate synthesis*; Harwood Academic Publishers: Amsterdam, The Neterhelands, 1996.
(8) Baty, J.; Sinnott, M. L. *Chem. Commun.* **2004**, No. 7, 866–867.
(9) Clark, C. R.; Hay, R. W.; Dea, I. C. M. *J. Chem. Soc., Chem. Commun.* **1970**, No. 13, 794–5.

Published on Web 02/18/2010

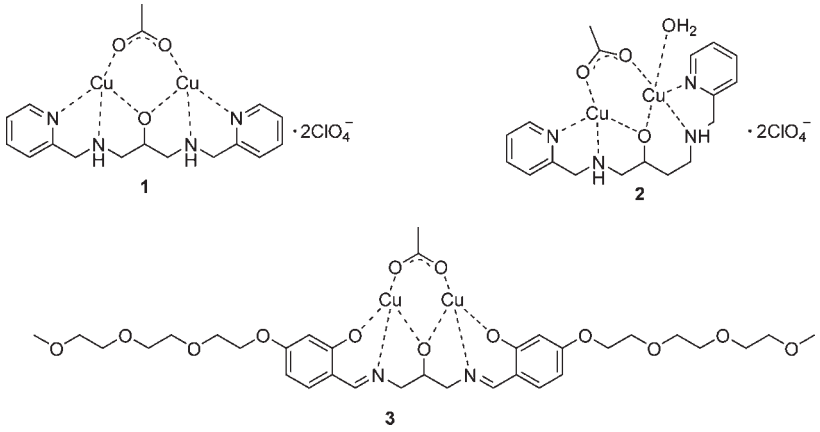

Figure 1. Structures of binuclear copper(II) complexes **1**, **2**, and **3**.

Scheme 1. Synthesis of Asymmetric Complex **2**

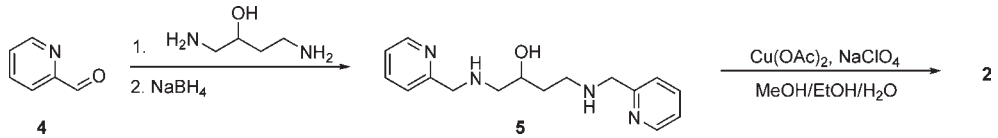

diperchlorate, Cu_2bpdpo (**1**),[10−12] its asymmetric analogue *N*,*N*′-{bis(2-pyridylmethyl)-1,4-diaminobutan-2-ol}ato dicopper(II) (μ-acetato) diperchlorate, Cu_2bpdbo (**2**), and a symmetric salicylaldehyde-based analogue *N*,*N*′-{1,3-bis[{2-hydroxy-4-[2-(2-methoxyethoxy)-ethoxy]-ethoxy}benzylideneamino]-propan-2-ol}ato dicopper (μ-acetate), Cu_2TEGbsdpo (**3**),[12,13] were employed toward this end (Figure 1).

Results and Discussion

Complex Structures in the Solid State. To elucidate the connection between intermetallic distance and catalytic performance during glycoside hydrolysis, the binuclear copper(II) complexes **2** and **3** were studied in the solid state via X-ray diffraction of single crystals. The intermetallic distances and the geometry of the backbone ligands around the metal cores were determined and compared to the structural data of **1a**,[14] which is a known phosphate analogue of **1**; our efforts to crystallize **1** itself were futile, its synthesis and the sugar binding ability were described previously.[10−12,22,23]

Both complexes, **1** and **1a**,[14] possess the same backbone ligand and differ only in the bridging counteranion (**1**: acetate; **1a**:[14] diphenylphosphate). The structure analyses of binuclear Cu(II) complexes with related backbone ligands and monobridging acetato groups show intramolecular Cu···Cu distances of 3.418−3.541 Å.[15−19] Thus, the distance between the Cu(II) ions in **1a** (3.499(1) Å)[14] is within this typical range for acetato-bridged binuclear complexes, but is considerably longer than in other phosphato-bridged complexes, for example, $[Cu_2(L1)(O_2P(OAr))](ClO_4)_2$, HL1 = 2,6-bis[bis(2-pyridylethyl)-aminomethyl]phenol; Ar = *p*-nitrophenol, Cu···Cu = 3.001 Å;[20,21] We consequently assume that **1** behaves like other acetato-bridged complexes which renders the geometry of the Cu(II) ions and the intramolecular Cu···Cu distances in the acetato-bridged complex **1** (discussed herein) and the known diphenylphosphato-bridged complex **1a**[14] comparable.

Complex **2** was prepared by condensing commercially available 2-pyridine carboxaldehyde (**4**) with 1,4-diaminobutan-2-ol at ambient temperature following a protocol for the preparation of **1** that we developed previously (Scheme 1).[10−12,22,23] The Schiff-base ligand obtained was reduced in situ with sodium borohydride supplying the pentadentate ligand *N*,*N*′-bis(2-pyridylmethyl)-1,4-diaminobutan-2-ol, bpdbo, (**5**). The coordination of copper(II) acetate monohydrate to **5** in the presence of sodium perchlorate in an aqueous ethanol-methanol solution yielded blue crystals of **2** after slow evaporation of the solvent.

Elemental analysis suggests a composition of $C_{18}H_{26}Cl_2Cu_2N_4O_{12}$ for **2**, while the complex formation between **5** and copper(II) acetate monohydrate is evident from infrared spectra (see Supporting Information). The C−H deformation vibrations of the pyridyl groups shift from 1475 and 1433 cm^{-1} in **5** to 1480 and 1451 cm^{-1} in **2**,

(10) Striegler, S. *Tetrahedron* **2006**, *62*(39), 9109–9114.
(11) Striegler, S.; Dittel, M. *J. Am. Chem. Soc.* **2003**, *125*(38), 11518–11524.
(12) Striegler, S.; Gichinga, M. G. *Chem. Commun.* **2008**, 5930–5932.
(13) Striegler, S.; Gichinga, M. G.; Dittel, M. *Org. Lett.* **2008**, *10*(2), 241–244.
(14) Gajda, T.; Jancso, A.; Mikkola, S.; Loennberg, H.; Sirges, H. *J. Chem. Soc., Dalton Trans.* **2002**, No. 8, 1757–1763.
(15) Siluvai, G. S.; Murthy, N. N. *Polyhedron* **2009**, *28*(11), 2149–2156.
(16) Yamaguchi, K.; Akagi, F.; Suzuki, S.; Fujinami, S.; Suzuki, M.; Shionoya, M. *Chem. Commun.* **2001**, No. 4, 375–376.
(17) Murthy, N. N.; Karlin, K. D.; Bertini, I.; Luchinat, C. *J. Am. Chem. Soc.* **1997**, *119*(9), 2156–2162.
(18) Nie, H.; Aubin, S. M. J.; Mashuta, M. S.; Porter, R. A.; Richardson, J. F.; Hendrickson, D. N.; Buchanan, R. M. *Inorg. Chem.* **1996**, *35*(11), 3325–34.
(19) McKee, V.; Zvagulis, M.; Dagdigian, J. V.; Patch, M. G.; Reed, C. A. *J. Am. Chem. Soc.* **1984**, *106*(17), 4765–72.
(20) Murugavel, R.; Pothiraja, R.; Gogoi, N.; Clerac, R.; Lecren, L.; Butcher, R. J.; Nethaji, M. *Dalton Trans.* **2007**, No. 23, 2405–2410.
(21) Siluvai, G. S.; Murthy, N. N. *Inorg. Chim. Acta* **2009**, *362*(9), 3119–3126.
(22) Gichinga, M. G.; Striegler, S. *Tetrahedron* **2009**, *65*(25), 4917–4922.
(23) Striegler, S. *Anal. Chim. Acta* **2005**, *539*(1−2), 91–95.

respectively, while the N−H deformation vibration of the secondary amino groups changes from 1592 to 1612 cm^{-1}. The aliphatic C−O stretching vibrations found at 1048 cm^{-1} in **5** cannot be unambiguously assigned to a vibration in **2** and overlap badly with very strong perchlorate stretching vibrations at 1098 cm^{-1}. Nevertheless, comparable assignments of the observed infrared bands were made previously for related complexes.[24]

The structural study of **2** reveals an intermetallic Cu···Cu distance of 3.39 Å and a tridentate N_2O donor set of **5** to each metal ion.[24] Both Cu(II) ions, Cu(1) and Cu(2), are bridged by the endogenous μ-alkoxo oxygen atom O(11) of **5** and the oxygen atoms O(9) and O(10) of an exogenous acetate group (Figure 2).

The equatorial donor atoms N(2)−N(1)−O(11)−O(10) around Cu(1) strongly deviate from their best plane leading to significant torsion of the N_2O_2 donor set by 19.2°. The coordination sphere of Cu(1) is completed by the oxygen atom O(3) of a perchlorate counteranion that is weakly bound in an axial position. The average Cu−N and Cu−O distances in the equatorial plane of Cu(1) are 1.998 and 1.922 Å, respectively. These distances are similar to the corresponding averages in the symmetric analogue **1a**.[14] The distance of Cu(1) to the axial perchlorate oxygen atom O(3) is 2.542 Å in **2**, and comparable to the average distance observed for weakly coordinating perchlorate oxygen atoms in **1a**.[14]

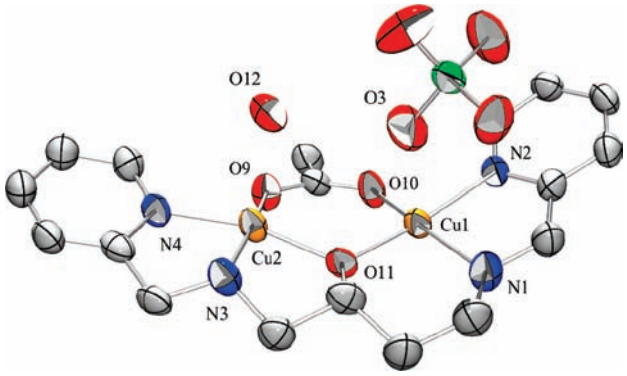

Figure 2. ORTEP3[25]-POV Ray representation for the structure of **2**, Cu_2bpdbo, depicted in ellipsoids with 60% probability; carbon atoms in gray, copper atoms in yellow, oxygen atoms in red, nitrogen atoms in blue, and chlorine atoms in green; hydrogen atoms and a second perchlorate anion are omitted for clarity.

The second metal ion, Cu(2), is bound in a square pyramidal environment with a N_2O_3 donor set consisting of ligand **5**, the exogenous acetate group, and the oxygen atom O(12) of a strongly coordinated water molecule in axial position. By contrast, the basal plane N(4)−N(3)−O(11)−O(9) is nearly perfect, and Cu(2) lies 0.129 Å above this plane; again, this displacement is similar to that in **1a**.[14] The angle Cu(1)−O(11)−Cu(2) is 123.5(2)° in **2**, and is considerably smaller than in **1a** (132.9(2)°).[14] This observation is ascribed to the distortion of **2** because of the asymmetry of ligand **5**. The structure of **2** in the solid state is accordingly determined as $[Cu_2(\mathbf{5}_{-H})(OAc)(H_2O)(ClO_4)]ClO_4$. The distortion of **2** decreases the intermetallic distance (Cu···Cu: 3.39 Å) by about 0.1 Å in comparison to **1a** (Cu···Cu: 3.499(1) Å),[14] but remains in the typical distance observed for other monobridged binuclear complexes.[15−19] While this small difference in the distance between the two Cu(II) ions alone might only have a minor effect on the catalytic turnover, the overall distorted geometry of **2** in comparison to **1a** might have a profound effect on a putative use of the complexes as transition metal catalysts. Selected bond distances, angles, and dihedral angles of **2** are listed in Table 1.

Prior to investigating the relevance of the intermetallic distance and the overall complex geometry for catalytic hydrolysis reactions, we prepared a symmetric Schiff-base complex **3** (Figure 1) derived from salicylaldehyde derivatives to alter the hydrogen donor and acceptor properties of the ligand backbone while preserving the geometry of the coordination sites of the Cu(II) ions in comparison to **1**. Diffraction-quality single crystals of **3** were not obtained despite all efforts; the flexibility of its water solubility-enhancing triethylene glycol side chains most likely prevents crystallization. Instead, complex **3a** with a methoxyethylene glycol side chain was prepared and examined. This minor alteration at the periphery of the ligand backbone is very unlikely to affect the geometry of the binuclear metal core in **3a** versus **3**. A comparison of the structure−activity relationship for complexes **1** and **3**, however, will provide valuable insights for the catalyst design and the choice of electron donating or withdrawing backbone ligands (see below) at a given intermetallic distance.

The synthesis of **3a** followed a protocol for the regioselective alkylation of hydroxysalicylaldehydes that we

Table 1. Selected Bond Lengths *l* [Å], Angles Φ [deg] and Torsion Angles τ [deg] for **2**

distance *l*	[Å]	angle Φ	[deg]	dihedral angle τ	[deg]
Cu(1)−O(11)	1.908(3)	O(11)−Cu(1)−O(10)	94.7(1)	N(3)−Cu(2)−O(11)−Cu(1)	159.4
Cu(1)−O(10)	1.935(3)	O(11)−Cu(1)−N(1)	97.1(2)	N(4)−Cu(2)−O(11)−Cu(1)	162.7
Cu(1)−N(1)	1.987(4)	O(10)−Cu(1)−N(1)	162.2(2)	N(1)−Cu(1)−O(11)−Cu(2)	164.2
Cu(1)−N(2)	2.008(4)	O(11)−Cu(1)−N(2)	170.5(2)	N(2)−Cu(1)−O(11)−Cu(2)	80.8
Cu(2)−O(9)	1.929(3)	O(10)−Cu(1)−N(2)	88.5(1)		
Cu(2)−O(11)	1.941(3)	N(1)−Cu(1)−N(2)	81.8(2)		
Cu(2)−N(3)	1.985(4)	O(9)−Cu(2)−O(11)	98.7(1)		
Cu(2)−N(4)	2.002(4)	O(9)−Cu(2)−N(4)	91.4(1)		
Cu(2)−O(12)	2.303(4)	O(9)−Cu(2)−N(3)	167.2(2)		
Cu(1)···O(3)	2.542	O(11)−Cu(2)−N(4)	165.3(1)		
Cu(1)···Cu(2)	3.390	O(11)−Cu(2)−N(3)	86.3(2)		
		N(3)−Cu(2)−N(4)	81.8(2)		
		O(9)−Cu(2)−O(12)	92.7(1)		
		O(11)−Cu(2)−O(12)	98.2(2)		
		N(3)−Cu(2)−O(12)	98.3(2)		
		N(4)−Cu(2)−O(12)	91.8(1)		
		Cu(1)−O(11)−Cu(2)	123.5(2)		

Scheme 2. Synthesis of Schiff Base Complex **3a**

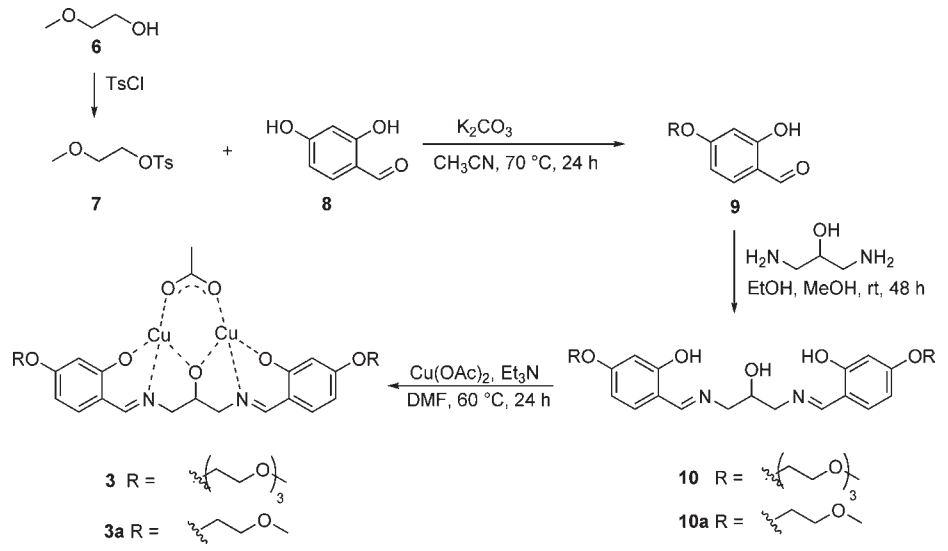

developed earlier;[22] in short, the hydroxyl group of 2-methoxyethanol (**6**) was activated by tosylation yielding **7**, which was subsequently reacted with 2,4-dihydroxybenzaldehyde (**8**) in a Williamson ether synthesis providing a regioselectively alkylated aldehyde **9**. Condensation of **9** with 1,3-diaminopropanol supplied pentadentate ligand *N*,*N*′-1,3-bis[{2-hydroxy-4-[2-(methoxyethoxy)]}-benzylideneamino]propan-2-ol, EGbsdpo, (**10a**) (Scheme 2). The reaction of **10a** with copper(II) acetate monohydrate in the presence of triethylamine yielded a green solid that was crystallized from ethanol to obtain **3a** after slow evaporation of the solvent.

Elemental analysis revealed the composition of complex **3a** as $C_{25}H_{31}Cu_2N_2O_9$. Infrared spectra showed a shift of the azomethine band in **10a** upon coordination of copper(II) acetate monohydrate from 1634 cm^{-1} to 1630 cm^{-1} in **3a**. Similarly, the phenoxy C−O stretch vibration band is shifted from 1116 cm^{-1} in **10a** to 1123 cm^{-1} in **3a** (see Supporting Information). Comparable shifts have been observed for the formation of other Schiff-base complexes previously.[26]

The structure analysis of **3a** by X-ray diffraction indicates square planar coordination environments for both Cu(II) ions, which are bridged by an endogenous μ-alkoxo oxygen atom of **10a** and an exogenous μ-1,3-coordinating acetate group, providing N_1O_3 donor sets (Figure 3). Very similar bond lengths and bond angles are reported for related binuclear Cu(II) complexes derived from other salicylaldehyde (derivatives) and 1,3-diaminopropanol.[27] A discussion of the structural features of **3a** is consequently shortened herein. Notably, the intermetallic Cu···Cu bond distance in **3a** is 3.506 Å and thus comparable to **1a**[14] and **1** (see above) despite the different electronic nature of the backbone ligand **10a** in comparison to **11**, *N*,*N*′-1,3-bis[(pyridin-2-ylmethyl)amino]propan-2-ol (bpdpo, backbone ligand of **1a**[14] and **1**). Selected bond angles, distances, and torsion angles are listed in Table 2. The structure of Cu_2(EGbsdpo) (**3a**) in the solid state is confirmed as Cu_2(**10a**$_{-3H}$)(OAc).[28]

Complex Structures in Aqueous Solution. The composition of complexes **2** and **3** was determined in aqueous solution prior to investigating a potential glycosidase-like activity of all dinuclear copper(II) complexes. Toward this end, spectrophotometric titrations using the method from Zuberbühler et al. were employed using the global analysis model.[29] The compositions of **1** in water and of **3** in aqueous methanol were established previously.[11,12,14]

For complex **3**, a solution of the water-soluble ligand **10** and copper(II) acetate monohydrate (molar ratio 1:2) was titrated with a sodium hydroxide solution from pH 4 to 13. The water-soluble ligand **10** (L = TEGbsdpo) is an analogue of **10a** (L = EGbsdpo) and different only in the length of its ethylene glycol side chains at the periphery of the ligand. The pentadentate ligands **10** and **10a** will therefore provide identical metal ion coordination sites in the complexes **3** and **3a**. From the alteration of the UV/vis spectra upon base addition, the distribution of species was computed (Figure 4).[29]

The titration experiment revealed the formation of a mononuclear copper(II) complex **3b** $[CuL]^{2+}$ between pH 5 and 7, whereas several binuclear complexes are observed at alkaline pH. A binuclear complex **3c**,

(24) Striegler, S.; Dittel, M. *Inorg. Chem.* **2005**, *44*(8), 2728–2733.
(25) Farrugia, L. J. *J. Appl. Crystallogr.* **1997**, *30*(5, Pt. 1), 565.
(26) Jana, S.; Dutta, B.; Bera, R.; Koner, S. *Langmuir* **2007**, No. 23, 2492–2496.
(27) Butcher, R. J.; Diven, G.; Erickson, G.; Jasinski, J.; Mockler, G. M.; Pozdniakov, R. Y.; Sinn, E. *Inorg. Chim. Acta* **1995**, *239*(1−2), 107–16.

(28) X-ray structural analyses: Cu_2(EGbsdpo)(OAc) (**3a**):$C_{25}H_{31}Cu_2N_2O_9$, green rectangular, crystal dimensions 0.128 × 0.076 × 0.024 mm, triclinic, $P\bar{1}$, Z = 2, a = 6.381(2), b = 10.723(4), c = 19.732(7) Å, α = 94.606(7)°, β = 91.898(7)°, γ = 107.159(7)°, V = 1283.5(8) Å^3 (T = 193 K), μ = 17.14 cm^{-1}, R1 = 0.0523, ωR2 = 0.1151; Cu_2(bpdbo)(OAc)-$(ClO4)_2$ (**2**): $C_{18}H_{26}Cl_2Cu_2N_4O_{12}$, blue platelet, crystal dimensions 0.304 × 0.250 × 0.168 mm, monoclinic, $P21/n$, Z = 4, a = 15.0763(17), b = 12.2502(14), c = 15.3221(18) Å, β = 116.020(2)°, V = 2543.0(5) Å^3 (T = 153 K), μ = 19.51 cm^{-1}, R1 = 0.0584, ωR2 = 0.1830; Bruker APEX CCD diffractometer: θ_{max} = 56.62° (**3a**) and 56.68° (**2**), MoK_α, λ = 0.71073 Å, 0.3° ω scans, 13126 (**3a**) and 24008 (**2**) reflections measured, 6310 (**3a**) and 6303 (**2**) independent reflections all of which were included in the refinement. The data was corrected for Lorentz-polarization effects and for absorption (SHELXPREP), solutions were solved by direct methods, anisotropic refinement of F^2 by full-matrix least-squares, 343 parameters. Further details of the crystal structure investigations may be obtained from the CIF files.

(29) Binstead, R. A.; Jung, B.; Zuberbühler, A. D. *SPECFIT/32 Global Analysis System, 3.0*; Spectrum Software Associates: Marlborough, MA, 2000.

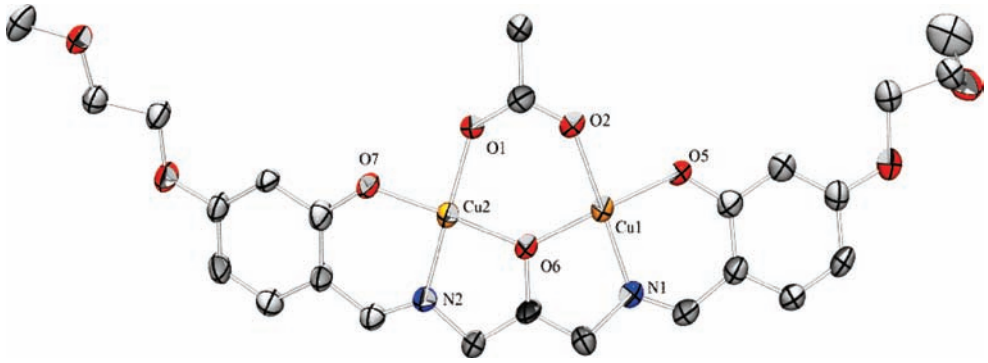

Figure 3. ORTEP[25]−POV ray representation for the structure of **3a**, Cu_2(EGbsdpo), depicted in ellipsoids with 60% probability; carbon atoms in gray, copper atoms in yellow, oxygen atoms in red, nitrogen atoms in blue, and chlorine atoms in green; all hydrogen atoms are omitted for clarity.

Table 2. Selected Bond Lengths [Å] and Bond Angles [deg] for Complex **3a**, Cu_2EGbsdpo

distance l	[Å]	angle Φ	[deg]	dihedral angle τ	[deg]
Cu(1)−O(5)	1.897(3)	O(5)−Cu(1)−O(6)	173.7(1)	N(2)−Cu(2)−O(6)−Cu(1)	179.81
Cu(1)−O(6)	1.910(3)	O(5)−Cu(1)−N(1)	93.6(1)	N(1)−Cu(1)−O(6)−Cu(2)	166.48
Cu(1)−N(1)	1.921(3)	O(6)−Cu(1)−N(1)	84.8(1)		
Cu(1)−O(2)	1.931(3)	O(5)−Cu(1)−O(2)	87.8(1)		
Cu(2)−O(7)	1.893(2)	O(6)−Cu(1)−O(2)	94.5(1)		
Cu(2)−O(6)	1.921(2)	N(1)−Cu(1)−O(2)	173.6(2)		
Cu(2)−N(2)	1.925(3)	O(7)−Cu(2)−O(6)	175.2(1)		
Cu(2)−O(1)	1.942(3)	O(7)−Cu(2)−N(2)	93.3(1)		
Cu(1)···Cu(2)	3.506	O(6)−Cu(2)−N(2)	83.9(1)		
		O(7)−Cu(2)−O(1)	87.6(1)		
		O(6)−Cu(2)−O(1)	94.6(1)		
		N(2)−Cu(2)−O(1)	171.3(1)		
		Cu(1)−O(6)−Cu(2)	132.5(1)		

$[Cu_2L_{-2H}]^{2+}$, dominates in solution above pH 6.6 and is further deprotonated above pH 8.6 forming **3d**, $[Cu_2L_{-3H}]^{+}$; the species **3e**, $[Cu_2L_{-3H}(OH)]$, dominates above pH 11.2. Plausible structures for the complexes **3b**−**3e** are suggested in Scheme 3; binding constants and species considered during computation are given in the Supporting Information. The pK_a for the coordination of water is calculated from these values as 11.66.

To characterize the composition of the asymmetric complex **2** in aqueous solution, a solution of ligand **5** (L = bpdbo) and copper(II) acetate monohydrate was titrated with base as described for **3** (vide infra). The species distribution data reveal the presence of free Cu(II) ions and **5**, and the formation of a mononuclear species $[CuL]^{2+}$ (**2a**) between pH 5 and 8 (Figure 5).

The formation of a binuclear species $[Cu_2L_{-H}]^{3+}$ (**2b**) competing with **2a** is noted above pH 6. Further deprotonation of **2b** in its backbone ligand **5** in alkaline pH is unlikely due to the high pK_a values typically observed for secondary amines,[30] although equilibrium structures may still exist. Any subsequent loss of protons in alkaline solution is thus ascribed to the deprotonation of water molecules coordinating to the metal center of **2**.

The loss of a proton of a water molecule coordinating to $[Cu_2L_{-H}]^{3+}$ above pH 9.5 results in the formation of a $[Cu_2L_{-H}(OH)]^{2+}$ species (**2c**), which is the predominant form of **2** above pH 10.7 (Scheme 4). The pK_a for the water coordination is calculated as 10.66 from the

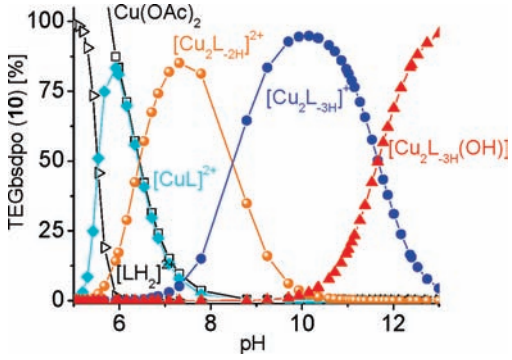

Figure 4. Distribution of species for binuclear copper(II) complex **3** derived from **10** and $Cu(OAc)_2 \cdot H_2O$ (molar ratio = 1:2) in aqueous solution between pH 5 and 13 at 30 °C.

binding constants of **2b** and **2c**. Further deprotonation of $[Cu_2L_{-H}(OH)]^{2+}$ above pH 13 leads to the formation of $[Cu_2L_{-H}(OH)_2]^{+}$ (**2d**). The large intermetallic Cu···Cu distance (3.39 Å) in **2** suggests terminal coordination of the resulting hydroxide ions to one of the Cu(II) ions rather than μ-coordination to both.[14,31−33]

In view of the subsequent evaluation of the binuclear complexes as catalysts for the hydrolysis of glycosides, the speciation data also reveal the composition of the complexes and a possible catalytic form under the chosen conditions (CAPS buffer, pH 10.5). Accordingly,

(30) Martell, A. E.; Smith, R. M. *NIST - Critically selected stability constants of metal complexes database*, Version 5.0; U. S. Department of Commerce, National Institute of Standards and Technology: Gaithersburg, MD, 1998.

(31) Frey, S. T.; Murthy, N. N.; Weintraub, S. T.; Thompson, L. K.; Karlin, K. D. *Inorg. Chem.* **1997**, *36*(6), 956–957.

(32) Gajda, T.; Kramer, R.; Jancso, A. *Eur. J. Inorg. Chem.* **2000**, No. 7, 1635–1644.

(33) Mazurek, W.; Berry, K. J.; Murray, K. S.; O'Connor, M. J.; Snow, M. R.; Wedd, A. G. *Inorg. Chem.* **1982**, *21*(8), 3071–80.

Scheme 3. Structures for the Copper(II) Species **3b**−**3e** Derived from **10** and $Cu(OAc)_2 \cdot H_2O$ between pH 4 and 13

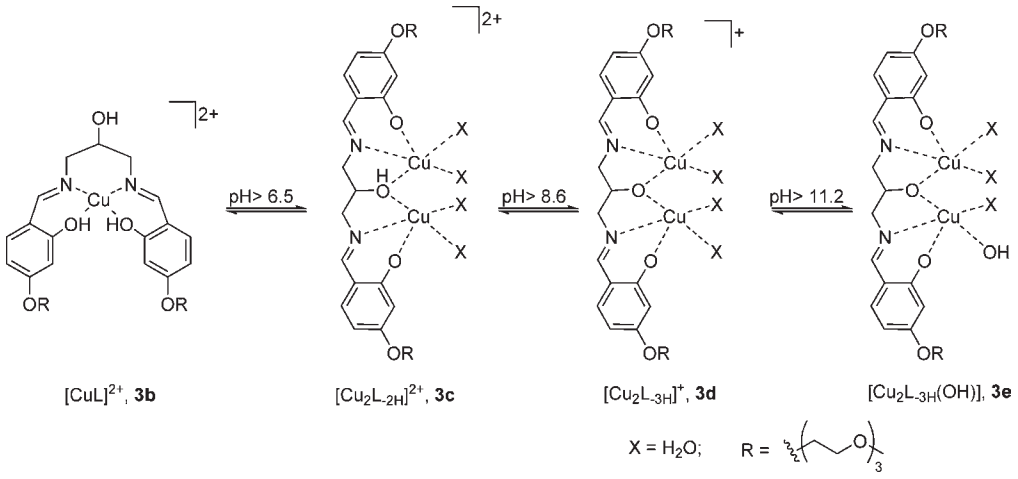

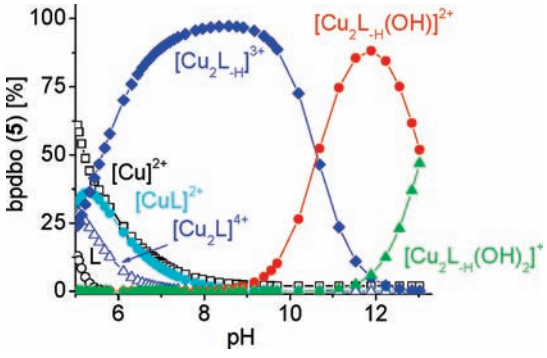

Figure 5. Distribution of species derived from **5** and $Cu(OAc)_2 \cdot H_2O$ (molar ratio 1: 2) in aqueous solution between pH 5 and 13 at 30 °C.

complex **1** exists primarily as $[Cu_2(\mathbf{11}_{-H})(OH)]^{2+}$ species (88%), whereas the remaining ligand is forming a Cu_2-$[(\mathbf{11}_{-H})(OH)_2]^{+}$ species, with **11** (bpdpo) as backbone ligand of **1**.[11,14] Both forms may be catalytically active. By contrast, the asymmetric analogue **2** exists predominantly as $[Cu_2(\mathbf{5}_{-H})]^{3+}$ species (56%) and to about 44% as $[Cu_2(\mathbf{5}_{-H})(OH)]^{2+}$ species, with **5** (bpdbo) as backbone ligand of **2**. Complex **3** forms mainly a $[Cu_2(\mathbf{10}_{-3H})]^{+}$ species (93%) at the given pH, while the $[Cu_2(\mathbf{10}_{-3H})$-(OH)] species exists in less than 7%, with **10** (TEGbsdpo) as backbone ligand of **3**. Hypothesizing that the hydrolysis of glycosides requires the presence of a hydroxyl group-containing species, the apparent catalytic activity of **1** should be higher than that of **2** or **3** in 3-(cyclohexylamino)-1-propanesulfonic acid (CAPS) buffer at pH 10.5.

Hydrolysis of a Model Glycoside. To probe the structural and electronic effects of the ligand backbone on the catalytic performance of the binuclear Cu(II) complexes, the ability of **1**, **2**, and **3** to hydrolyze *p*-nitrophenyl-α-D-galactopyranoside (**12**) in CAPS buffer at pH 10.5 was studied as a model reaction. The intermetallic distances in the binuclear complexes are comparable (~3.5 Å) as revealed by the discussion on their structure analyses (vide infra). Any difference in the catalytic performance of the complexes is therefore related to the electronic features of the ligand backbones and, consequently, to the species derived therefrom. A comparison of the catalytic performance of complexes **1** and **2** will furthermore disclose the influence of an overall planar (**1**) and distorted (**2**) complex geometry on the Lewis acidity of the metal centers.

In a model reaction, the catalytic hydrolysis of **12** was monitored by the formation of the yellow *p*-nitrophenoxide anion using UV/vis spectroscopy at 410 nm (Scheme 5). The reaction depends linearly on the concentration of the catalyst under the provided conditions (see Supporting Information).

Attempts to increase the substrate concentration to reach saturation of the catalytic sites were limited by the solubility of **12** in aqueous solution. Nevertheless, pseudo-first order conditions were provided with excess substrate in concentrations between 5 and 50 mM and a catalyst concentration of 0.1 mM. The hydrolysis of **12** was followed under these conditions for 26 h without any evidence for catalyst deactivation by product inhibition (see Supporting Information). The related substrates *p*-nitrophenyl-β-D-galactopyranoside (**13**), *p*-nitrophenyl-α-D-glucopyranoside (**14**), and *p*-nitrophenyl-β-D-glucopyranoside (**15**) were found to have an even lower solubility in aqueous solution than **12**, which limited their examination to concentrations between 5 and 35 mM. When rate constants (k_{cat}) and Michaelis−Menten constants (K_M) for the catalytic hydrolysis of **12**−**16** could not be obtained by a non-linear regression fit of the *p*-nitrophenolate formation (Table 3), the catalytic efficiency (k_{cat}/K_M) was estimated from a linear fit of the data.

All binuclear complexes show significant accelerations of the hydrolysis of **12** (by at least a factor of 10^3). Of the three complexes, the catalytic efficiency (k_{cat}/K_m) of **1** is about twice that of **2** and about 2.5 times that of **3**. The catalytic efficiency of **1** to catalyze the hydrolysis of **12** is about 2-fold higher than the cleavage of the glycosidic bonds in **13**, **14**, or **15**; a similar trend is observed when using **2** as catalyst under otherwise identical conditions. The catalytic efficiency of **2** during the catalytic hydrolysis of *o*-nitrophenyl-α-D-galactopyranoside (**16**) is about 6-fold lower than for **12** because of increased autocatalytic hydrolysis of this substrate. These results overall suggest a slight preference for a pyridyl ring (**1** and **2**) over a phenoxy group (**3**) in the ligand framework of the catalyst, and for a symmetrical (**1**) over an unsymmetrical (**2**) backbone ligand for the future design of

Scheme 4. Structures for Copper(II) Species **2a**−**2d** Derived from **5** and $Cu(OAc)_2 \cdot H_2O$ between pH 5 and 13

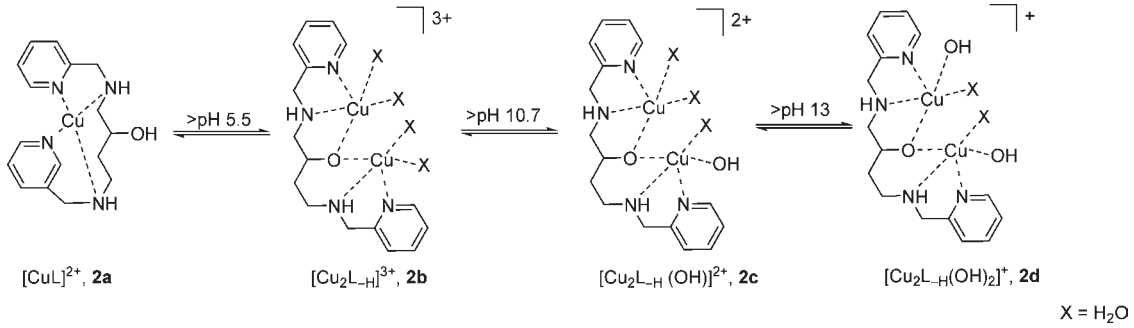

$[CuL]^{2+}$, **2a** $[Cu_2L_{-H}]^{3+}$, **2b** $[Cu_2L_{-H}(OH)]^{2+}$, **2c** $[Cu_2L_{-H}(OH)_2]^{+}$, **2d**

Scheme 5. Catalytic Hydrolysis of *p*-Nitrophenyl-α-D-galactopyranoside (**12**)

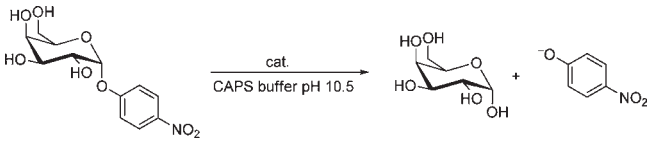

binuclear complexes for the hydrolysis of glycosides. The electronic features of the ligand backbone control the Lewis acidity of the metal core in **1**, **2**, and **3** and determine the amount of the resulting catalytically active species containing deprotonated water.

In combination with the speciation data, we suggest $[Cu_2(\mathbf{11}_{-H})(OH)]^{2+}$, $[Cu_2(\mathbf{5}_{-H})(OH)]^{2+}$, and $[Cu_2(\mathbf{10}_{-3H})(OH)]$ as the catalytic active forms of **1**, **2**, and **3** at pH 10.5, respectively. However, the speciation data of **2** and **3** indicate the presence of $[Cu_2(\mathbf{5}_{-H})]^{3+}$ and $[Cu_2(\mathbf{10}_{-3H})]^{+}$ as major species under these conditions (vide infra). To clarify the role of the major species versus a putative catalytically active minor species, the catalytic hydrolysis of **12** by **2** and **3** was additionally studied in borate and TAPS buffer at pH 9. Under these conditions, complex **2** exists as $[Cu_2(\mathbf{5}_{-H})]^{3+}$ (97.5%) and as $[Cu_2(\mathbf{5}_{-H})(OH)]^{2+}$ (2.5%) species (Figure 5). The catalytic hydrolysis of **12** is slowed down by about 1.5 orders of magnitude (Table 3, entry 11) indicating a decrease in the amount of the catalytically active species. Similarly, complex **3** exists as $[Cu_2(\mathbf{10}_{-3H})]^{+}$ species (73.1%), $[Cu_2(\mathbf{10}_{-2H})]^{+}$ species (26.6%) and as hydroxyl group containing species $[Cu_2(\mathbf{10}_{-3H})(OH)]$ (0.3%) (Figure 4). At pH 9, the catalytic hydrolysis of **12** proceeds in the same order of magnitude as the background reaction (without catalyst) even when the concentration of **3** is increased by 10-fold. Thus, the species $[Cu_2(\mathbf{5}_{-H})]^{3+}$ and $[Cu_2(\mathbf{10}_{-3H})]^{+}$ are not catalytically active despite their predominant presence at pH 10.5, and the catalytic hydrolysis of **12** is solely promoted by $[Cu_2(\mathbf{5}_{-H})(OH)]^{2+}$ and $[Cu_2(\mathbf{10}_{-3H})(OH)]$ as proposed above.

The catalytic hydrolysis of **12** by complex *N*,*N*′-1,3-bis[(pyridin-2-ylmethyl)amino]propan-2-ol copper(II) diperchlorate, Cubpdpo, **1b**,[14] was then studied to correlate the performance of the binuclear complex **1** to its mononuclear analogue. The hydrolysis of **12** is more than 1 order of magnitude slower with **1b**[14] than with **1** (Table 3) despite an increased catalyst concentration from 0.1 to 1 mM. This observation suggests a cooperative effect of both Cu(II) ions in the binuclear complexes during the transformation of **12**. An in situ prepared mononuclear complex **2a** derived from **5** and Cu(II) chloride behaves alike and promotes the hydrolysis of **12** about 1 order of magnitude slower than **2**. In related studies, binuclear transition metal complexes were shown to hydrolyze phosphodiesters and carboxylic acid esters very efficiently and superior to their mononuclear analogues.[14,34−42] Efforts to investigate the hydrolysis of **12** with free Cu(II) ions were futile as a precipitate (presumably Cu(II) hydroxide) is formed immediately upon dissolving Cu(II) chloride or Cu(II) acetate as catalyst precursor compounds in CAPS buffer at pH 10.5.

The presented experimental data allow some preliminary conclusions on the mechanism of the glycoside hydrolysis promoted by **1**, **2**, and **3**. The hydrolysis of the glycosides is linearly dependent on the catalyst concentration for all complexes under the conditions studied; however, an increase of the rate for the product formation is noted during prolonged reaction time and will be investigated in future studies (see Supporting Information). Saturation conditions allow treatment of the data as pseudo-first order kinetics and reveal the formation of a substrate-catalyst complex. The *p*-nitrophenolate product does not deactivate the catalyst during a 26 h time period. The hydrolysis proceeds at pH 10.5, but not at pH 9, indicating a contribution of the metal-bound hydroxide ion in base catalysis (Scheme 6). The catalyst may reform upon substitution of the coordinated sugar with water and subsequent proton loss in alkaline solution.

The hydrolysis of **12** catalyzed by **1** is overall about 11,000-fold accelerated over the background reaction (k_{cat}/k_{non}) at 30 °C in CAPS buffer. A comparable performance of artificial glycosidase mimics based on cyclodextrins has been reported; however, they require elevated temperatures (∼60 °C).[4] As complex **1** has been

(34) Gajda, T.; Duepre, Y.; Toeroek, I.; Harmer, J.; Schweiger, A.; Sander, J.; Kuppert, D.; Hegetschweiler, K. *Inorg. Chem.* **2001**, *40*(19), 4918–4927.
(35) Koevari, E.; Kraemer, R. *J. Am. Chem. Soc.* **1996**, *118*(50), 12704–12709.
(36) Yamada, K.; Takahashi, Y.-i.; Yamamura, H.; Araki, S.; Kawai, M.; Saito, K. *Chem. Commun.* **2000**, No. 14, 1315–1316.
(37) Feng, G.; Natale, D.; Prabaharan, R.; Mareque-Rivas, J. C.; Williams, N. H. *Angew. Chem., Int. Ed.* **2006**, *45*(42), 7056–7059.
(38) Jancso, A.; Mikkola, S.; Lonnberg, H.; Hegetschweiler, K.; Gajda, T. *Chem.—Eur. J.* **2003**, *9*(21), 5404–5415.
(39) Jurek, P. E.; Martell, A. E. *Chem. Commun.* **1999**, No. 16, 1609–1610.
(40) Selmeczi, K.; Giorgi, M.; Speier, G.; Farkas, E.; Reglier, M. *Eur. J. Inorg. Chem.* **2006**, No. 5, 1022–1031.
(41) Zhou, Y.-H.; Zhao, M.; Li, J.-H.; Mao, Z.-W.; Ji, L.-N. *J. Mol. Catal. A* **2008**, *293*(1−2), 59–64.
(42) Liu, C. T.; Neverov, A. A.; Brown, R. S. *J. Am. Chem. Soc.* **2008**, *130*(42), 13870–13872.

Table 3. Summary of Kinetic Parameters for the Catalytic Hydrolysis of the Glycopyranosides **12**−**16**;

entry	pH	cat	S	k_{cat} ($\times 10^{-4}$) [min^{-1}]	K_m [mM]	k_{non} ($\times 10^{-7}$) [M^{-1} min^{-1}]	k_{cat}/K_m ($\times 10^{-3}$) [M^{-1} min^{-1}]	k_{cat}/k_{non} [M]	$k_{cat}/(K_m \times k_{non})$
1	10.5	**1**	**12**	43.4 ± 9.6	213 ± 57	3.8	20.4	11,000	54,000
2	10.5	**1**	**13**	13.2 ± 2	80 ± 15	7.5	16.5	1,800	22,000
3	10.5	**1**	**14**	10.5 ± 4.5	138 ± 69	2.8	6.7	3,700	24,000
4	10.5	**1**	**15**	a	a	2.2	7.0	a	32,000
5	10.5	**1b**	**12**	3 ± 0.8	220 ± 70	3.8	1.4	800	3,700
6	10.5	**2**	**12**	21.4 ± 3.3	185 ± 35	3.8	11.6	5,600	30,000
7	10.5	**2**	**13**	20.0 ± 2.7	256 ± 38	7.5	7.8	2,700	10,000
8	10.5	**2**	**14**	2.4 ± 1	77 ± 12	2.8	3.1	860	11,000
9	10.5	**2**	**15**	5.0 ± 0.4	211 ± 20	2.2	2.4	2,300	11,000
10	10.5	**2**	**16**	2.5 ± 0.3	132 ± 20	32	1.9	80	600
11	9.0	**2**	**12**	a	a	0.6	0.7	a	12,000
12	10.5	**3**	**12**	12.7 ± 2.9	152 ± 43	3.8	8.4	3,300	22,000

[a] Not determined.

Scheme 6. Putative Mechanism for the Hydrolysis of **12** by **1** (n = 1) or **2** (n = 2)[a]

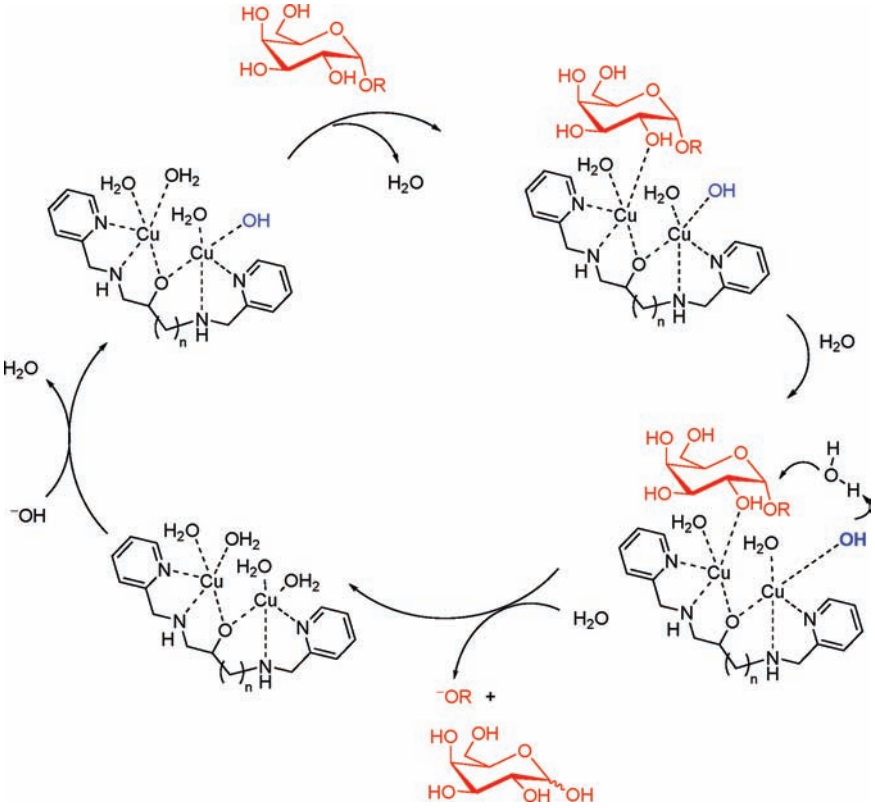

[a] $^{-}$OR = *p*-nitrophenolate.

previously shown to discriminate among carbohydrates,[11] a study to evaluate the *selective and catalytic* transformation of glycosides by binuclear copper(II) complexes will be topic of future investigations.

Conclusions. Three binuclear copper(II) complexes **1**, **2**, and **3** were synthesized and characterized in solid state by X-ray diffraction and by spectrophotometric titration in aqueous solution. The complexes show comparable intermetallic Cu···Cu distances despite electronically different backbone ligands. This observation is important for the comparison of distorted complex **2** to symmetric **1** during sugar binding and transformation. All complexes were found to moderately catalyze the hydrolysis of model glycosides in aqueous alkaline solution with up to 11,000-fold acceleration of the reaction over background. The glycoside hydrolysis is more than 1 order of magnitude slower when catalyzed by a mononuclear complex. Overall, the study has given very valuable insights and direction for the future design of transition metal complexes for the non-natural transformation of glycosides.

Experimental Section

Instrumentation. ^{1}H and ^{13}C NMR spectra were recorded on a Bruker AV 400 spectrometer (400.2 MHz for ^{1}H and 100.6 MHz for ^{13}C). Chemical shifts (δ) are expressed in parts per million and coupling constants (J) in hertz. Signal multiplicities are denoted as s (singlet), d (doublet), t (triplet), and m (multiplet). Deuterated chloroform was used as a solvent, and chemical shift values are reported relative to the residual signals of this solvent (δ = 7.24 for ^{1}H and δ = 77.0 for ^{13}C NMR). UV−vis spectra were recorded at 30.0 ± 0.1 °C over a range of 200−800 nm on a

Varian Cary 50 with WinUV Analysis Suite software, version 3.0, using disposable Brandtech macro cells (220−900 nm) of 1 cm thickness and 4.5 mL volume for the determination of the distribution of species. Disposable 1.5 mL semimicro Brandtech UV cuvettes (220−900 nm) of 10 mm light path with caps were used for the hydrolysis studies. The pH was measured using a Beckman Φ 250 pH meter equipped with refillable long Futura pH electrode of 0.7 mm thickness. The pH meter was calibrated before each set of readings (3-point calibration). The IR spectra were obtained on a Shimadzu IR Prestige-21 FT-IR spectrophotometer with IR solution software version 1.10 as thin films or KBr pellets (ν in cm^{-1}). X-ray diffraction data were collected on a Bruker SMART APEX CCD X-ray diffractometer. Samples for elemental analysis were sent to Atlantic Microlab Inc., Atlanta, GA. ESI-MS data were obtained on a VG Trio-2000 Fisons Instruments mass spectrometer with VG MassLynx software, version 2.00, or sent to the Laboratory for Biological Mass Spectrometry, Texas A&M University, College Station, TX, for analysis. Thin layer chromatography (TLC) was preformed on silica gel TLC plates from SORBENT Technologies, 200 μm, 4 × 8 cm, aluminum backed, with fluorescence indicator F_{254} with detection by charring with anthrone sulfate, and by UV light when applicable. Column chromatography was carried out using silica gel 60 as stationary phase from Silicycle (40−63 μm, 230−240 mesh). All melting points were recorded on a Mel-Temp melting point apparatus, and the values are uncorrected.

Chemicals. The ligand TEGbsdpo (**10**),[43] 2-hydroxy-4-(2-methoxyethoxy)benzaldehyde (**9**),[22] *N*,*N*′-{1,3-bis[(pyridin-2-ylmethyl)amino]propan-2-ol}ato dicopper(II) (μ-acetato) diperchlorate **1**,[44] *N*,*N*′-1,3-bis[(pyridin-2-ylmethyl)amino]propan-2-ol (bpdpo, **11**),[11,14] and 1,4-diaminobutan-2-ol dihydrochloride[45] were synthesized as described; 2-pyridine carboxaldehyde was obtained from Aldrich, distilled under reduced pressure and stored in the dark at 10 °C prior to use; 4-nitrophenol was obtained from Fluka. All other reagents were obtained from Fisher and Sigma−Aldrich and were used without further purification.

Synthesis of *N*,*N*′-1,3-bis{[2-hydroxy-4-(2-methoxyethoxy)]-benzylideneamino}propan-2-ol, EGbsdpo (10a). A solution of 1,3-diaminopropanol (115 mg, 1.24 mmol) in 10 mL of ethanol was added to a solution of 2-hydroxy-4-(2-methoxyethoxy)-benzaldehyde (**9**)[22] in 150 mL of ethanol/methanol (1/1, v/v) at ambient temperature and allowed to stir for 48 h. The resulting solution was evaporated to give a crude yellow product that was recrystallized from MeOH/EtOH (1/1 v/v) to give a yellow powder. Yield 23% (230 mg, 0.52 mmol); mp 120−121 °C; δ_H ($CDCl_3$) 8.16 (s, 2H, −CH=N−), 7.06 (d, 8.3, 2H, Ar*H*), 6.37 (m, 4H, Ar*H*), 4.15 (m, 1H, −C*H*OH−), 4.06 (t, 4.7, 4H, ArOCH_2−), 3.70 (m, 4H, −CH_2−), 3.59 (m, 2H, −CH_2−); δ_C ($CDCl_3$, 100.6 MHz) 166.1, 165.1, 163.2, 132.9, 112.2, 107.0, 101.8, 70.7, 70.2, 67.2, 61.3, 59.2; ν_{max} (KBr)/cm^{-1} 3356 (br, OH), 3075w (=CH arom.) 2880s (C−H), 1634v (C=N), 1115s (C−O). Positive ion ESI MS, calcd for $(C_{23}H_{30}N_2O_7 + H)^+$ 446.21, found 446.16.

***N*,*N*′-{1,3-bis{[2-hydroxy-4-(2-methoxyethoxy)]benzylideneamino}-propan-2-ol}ato dicopper (μ-acetate), Cu_2EGbsdpo, (3a).** A solution of copper(II) acetate monohydrate (100 mg, 0.5 mmol) in 10 mL of *N*,*N*-dimethylformamide (DMF) was added dropwise to a solution of **8** (110 mg, 0.25 mmol) in 30 mL of DMF. Triethyl amine (76 mg, 0.75 mmol) was then added, and the mixture allowed to stir at 60 °C for 24 h. The solution was then concentrated to half of its volume under vacuum at 60−70 °C, and the remaining solution kept in an open flask at ambient temperature. A green powder was isolated by filtration after 7 days and recrystallized from ethanol to obtain dark green crystals. Yield 44% (70 mg, 0.11 mmol). Found: C, 47.63; H, 4.80; N, 4.40%. $C_{25}H_{31}Cu_2N_2O_9$ requires: C, 47.62, H, 4.95, N, 4.44%; ν_{max} (KBr)/cm^{-1} 3455br (OH), 2905s (C−H), 1630v (C=N), 1128s (C−O).

***N*,*N*′-bis(2-pyridylmethyl)-1,4-diaminobutan-2-ol, bpdbo (5).** To a solution of 1,4-diaminobutan-2-ol dihydrochloride[45] (0.5 g, 2.82 mmol) in 20 mL of methanol was added a solution of sodium hydroxide (226 mg, 5.64 mmol) in 10 mL of methanol. The resulting solution was stirred at ambient temperature for 30 min and then filtered to remove precipitated NaCl. A solution of distilled 2-pyridine carboxaldehyde (0.6 g, 5.64 mmol) in 10 mL of methanol was added dropwise to the filtrate, and the resulting yellow solution stirred overnight at ambient temperature. Sodium borohydride (158 mg, 5.64 mmol) was then added in small portions after which the solution was refluxed for 1 h. It was then cooled to ambient temperature and evaporated to dryness by rotary evaporation. The crude product was dissolved in 20 mL of nanopure water and extracted using dichloromethane (2 × 50 mL). The separated organic layer was dried using anhydrous sodium sulfate and evaporated to obtain a yellow oil that was purified by chromatography on Sephadex LH-20-100 using methanol as eluent. Yield: 40% (320 mg, 1.1 mmol), yellow oil; R_f (SiO_2/MeOH): 0.3; δ_H (400.2 MHz, $CDCl_3$) 8.54 (m, 2H, −C*H* = N-), 7.75−7.55 (m, 2H, Ar*H*), 7.35−7.25 (m, 2H, Ar*H*), 7.22−7.06 (m, 2H, Ar*H*), 4.04−3.83 (m, 5H, ArOCH_2, −C*H*OH), 3.40−3.05 (m, 2H, NH), 3.04−2.76 (m, 2H, CH_2CH_2NH), 2.75−2.58 (m, 2H, CH_2NH), 1.77−1.52 (m, 2H, CH_2CH_2NH); δ_C (100.6 MHz, $CDCl_3$) 160.1, 159.3, 149.4, 149.3, 136.7, 136.6, 122.5, 122.3, 122.2, 122.0; IR (thin film on KBr disk) ν_{max}/cm^{-1} 3303br (OH), 3063w (N−H), 2927s, 2830s, 729s; HRMS calcd for $(C_{16}H_{22}N_4O + H)^+$ 287.1872; found 287.1874.

N*, *N*′-{bis(2-pyridylmethyl)-1,4-diaminobutan-2-ol}ato dicopper(II) (μ-acetato) Diperchlorate, Cu_2bpdbo, (2).** Copper(II) acetate monohydrate (1.4 g, 7.0 mmol) was dissolved in 10 mL of nanopure water and mixed with a solution of sodium perchlorate (2.8 g, 22.8 mmol) in 5 mL of water. The resulting solution was diluted with 140 mL of methanol and added to **5** (716 mg, 2.5 mmol) dissolved in 20 mL of ethanol at ambient temperature. The resulting solution immediately turned deep blue, and was concentrated to 30 mL under vacuum at 40 °C. The remaining solution was allowed to stand at ambient temperature for 4 days. A blue crystalline solid formed that was isolated by filtration, air-dried and not further purified. Yield 28% (480 mg, 0.7 mmol): ***Caution! *perchlorate salts are potentially explosive. However, we did not experience any difficulty in handling or drying the compound below 40 °C*; found: C, 31.52; H, 3.70; N, 8.09%. $C_{18}H_{26}Cl_2Cu_2N_4O_{12}$ requires C, 31.36; H, 3.95; N, 8.13%; ν_{max} (KBr)/cm^{-1} 3443br (OH) 3247w (N−H), 2930w (C−H), 1564s (N−H def), 1095s (C−O)

Species Distribution Studies. In a typical experiment, a 2 mL aqueous solution containing 1 mM copper(II) acetate monohydrate and 0.5 mM pentadentate ligand **5** or **10** were titrated with 10 μL of freshly prepared sodium hydroxide solution at 30.0 ± 0.1 °C. The ionic strength of the aqueous solution was maintained constant with 0.1 M $NaClO_4$. The pH was recorded after mixing the solutions thoroughly. UV−vis spectra were then taken as a function of the pH and the resulting data were computed by the global fitting model provided by the program Specfit.[29,46] The concentration of the sodium hydroxide solution titrated was increased gradually from 0.005 to 5 M.

Hydrolysis Studies. In a typical experiment, the concentration range of the substrate was 4−50 mM with a catalyst concentration of 0.1 mM in a solution with a total volume of 1 mL.

(43) Gichinga, M. G.; Striegler, S. *J. Am. Chem. Soc.* **2008**, *130*(15), 5150–5156.

(44) Mazurek, W.; Kennedy, B. J.; Murray, K. S.; O'Connor, M. J.; Rodgers, J. R.; Snow, M. R.; Wedd, A. G.; Zwack, P. *Inorg. Chem.* **1985**, *24* (20), 3258–64.

(45) Murase, I.; Ueno, S.; Kida, S. *Inorg. Chim. Acta* **1984**, *87*(2), 155–7.

(46) Gampp, H.; Maeder, M.; Meyer, C. J.; Zuberbuehler, A. D. *Talanta* **1985**, *32*(2), 95–101.

Experiments were conducted in 50 mM CAPS buffer at pH 10.5 or 50 mM borate buffer at pH 9. The reaction was monitored over time by formation of 4-nitrophenolate using UV−vis spectroscopy at 410 nm (or 450 nm for formation of 2-nitrophenolate).[47−49] The background reaction was performed in a similar manner but without addition of the catalyst. Stock solutions of the mononuclear complexes **1b** were prepared in situ from equimolar amounts of copper(II) chloride and the ligands bpdpo (**11**)[11,14] and bpdbo (**5**), respectively; stock solutions of the binuclear complexes **1**, **2**, and **3** were prepared by dissolving appropriate amounts of the isolated complexes. The extinction coefficient for the product formation was determined by a calibration curve and used to convert the absorbance of the reaction product into molar amounts (4-nitrophenolate in borate buffer: $\varepsilon = 16160\ M^{-1}\ cm^{-1}$; CAPS buffer: $\varepsilon = 16190\ M^{-1}\ cm^{-1}$; 2-nitrophenolate in CAPS buffer: $\varepsilon = 2310\ M^{-1}\ cm^{-1}$).

(47) Lai, Y.; Bakken, A. H.; Unadkat, J. D. *J. Biol. Chem.* **2002**, *277*(40), 37711–37717.
(48) Peretti, S. W.; Tompkins, C. J.; Goodall, J. L.; Michaels, A. S. *J. Membr. Sci.* **2002**, *195*(2), 193–202.
(49) Thompson, S. E.; Smith, M.; Wilkinson, M. C.; Peek, K. *Appl. Environ. Microbiol.* **2001**, *67*(9), 4001–4008.

Acknowledgment. A CAREER award from the National Science Foundation to S.S. (CHE-0746635) to support this work is gratefully acknowledged. The authors thank T. E. Albrecht-Schmitt for help with the structural analysis of complexes **2** and **3a**, and T. Webb for helpful discussion during the preparation of the manuscript.

Supporting Information Available: Kinetic profiles for the hydrolysis of **12** and **16** by **1**−**3**; ^{1}H and ^{13}C NMR spectra, IR spectra and MS chromatograms of **5** and **10a**. This material is available free of charge via the Internet at http://pubs.acs.org. CCDC 699736 (**2**), and 699735 (**3a**) contain supplementary crystallographic data and can be obtained free of charge from The Cambridge Crystallographic Data Centre via www.ccdc.cam.ac.uk/data_request/cif.